Author Manuscript

Author Manuscript

Author Manuscript

Author Manuscript

HHS Public Access

Author manuscript

Nat Immunol. Author manuscript; available in PMC 2012 January 01.

Published in final edited form as:

Nat Immunol. ; 12(7): 672–680. doi:10.1038/ni.2047.

The sphingosine 1-phosphate receptor S1P2 maintains germinal center B cell homeostasis and promotes niche confinement

Jesse A. Green[1], **Kazuhiro Suzuki**[1,*,‡], **Bryan Cho**[1,2,*], **L. David Willison**[3,*,‡], **Daniel Palmer**[3], **Christopher D.C. Allen**[1,‡], **Timothy H. Schmidt**[1], **Ying Xu**[1], **Richard L. Proia**[4], **Shaun R. Coughlin**[3], and **Jason G. Cyster**[1]

[1]Howard Hughes Medical Institute and Department of Microbiology and Immunology, University of California San Francisco, 513 Parnassus Ave., San Francisco, CA 94143-0414, USA

[2]Department of Dermatology, University of California San Francisco, 513 Parnassus Ave., San Francisco, CA 94143-0414, USA

[3]Cardiovascular Research Institute, University of California San Francisco, 600 16th Street S472D, San Francisco, CA 94143-2240, USA

[4]Genetics of Development and Disease Branch, National Institute of Diabetes and Digestive and Kidney Diseases, NIH, Bethesda, MD 20892, USA

Abstract

Sphingosine-1-phosphate receptor-2 (S1P2)-deficient mice develop diffuse large B cell lymphoma. However, the role of S1P2 in normal germinal center (GC) physiology is unknown. Here we show that S1P2-deficient GC B cells outgrow their wild-type counterparts in chronically-established GCs. We find that S1P2-, G12–G13- and p115RhoGEF-mediated antagonism of Akt regulates cell viability and is required for growth control in chronically proliferating GCs. We also find that S1P2 inhibits GC B cell responses to follicular chemoattractants and helps confine cells to the GC. Moreover, S1P2 overexpression promotes centering of activated B cells within the follicle. We suggest that by inhibiting Akt activation and migration, S1P2 helps restrict GC B cell survival and localization to an S1P-low niche at the follicle center.

Users may view, print, copy, download and text and data- mine the content in such documents, for the purposes of academic research, subject always to the full Conditions of use: http://www.nature.com/authors/editorial_policies/license.html#terms

Address correspondence to: J.G.C. (Jason.Cyster@ucsf.edu).

*These authors contributed equally to this study

‡Current addresses:

K. Suzuki: WPI Immunology Frontier Research Center, Osaka University, 3-1 Yamada-oka, Suita, Osaka 565-0871, Japan.

L. D. Willison: Semel Institute for Neuroscience and Human Behavior, University of California Los Angeles, 760 Westwood Plaza, Los Angeles, CA 90024, USA.

C.D.C. Allen: Sandler-Newmann Foundation, Department of Microbiology and Immunology, University of California San Francisco, 505 Parnassus Ave., San Francisco, CA 94143-0414, USA.

Please provide author contributions statement.

JAG, BC and JGC designed the experiments. JAG performed the bulk of the experiments and BC performed some of the early experiments. KS and JAG performed the imaging experiments. CDCA and YX performed the initial gene expression analysis. THS and JAG performed the PTEN inhibitor experiments. DW and SRC generated the G12-deficient mice and DP and SRC generated the *Gna12−/−Gna13f/fMx1cre* BM. RLP generated the S1P2-deficient mice. JAG, KS, BC, and JGC analyzed the data and JAG and JGC wrote the paper.

Author Manuscript Author Manuscript Author Manuscript Author Manuscript

Germinal centers (GCs) are induced in response to T-dependent antigens and support events necessary for antibody affinity maturation[1,2]. They arise in the center of B cell follicles and grow from small numbers of starting B cells to a size of ~10,000 cells in a matter of days. Despite the rapid growth rate, GC size is tightly regulated, even in mesenteric lymph nodes (mLNs) and Peyer's Patches (PPs) where the responses are chronically stimulated by gut flora[3]. Apoptosis is an integral part of GC growth control as GC B cells are highly prone to apoptotic cell death and are strongly dependent on CD40L and other trophic factors[4]. These factors act at least in part by maintaining expression of anti-apoptotic Bcl2-family proteins, including Mcl-1, that are critical for GC formation[5]. However, despite knowledge of key requirements for maintaining GC cell viability, the environmental cues involved in regulating GC size are not fully understood.

GCs are organized into dark and light zones by CXCL12 and CXCL13, respectively[6]. CXCL13 is present throughout the follicle and in the GC light zone; CXCL12 is present within the dark zone[6]. Despite the important roles of these chemokines, combined deficiency in the function of their receptors does not cause a complete loss of GC formation[6]. Another chemoattractant receptor, EBI2, is up-regulated in early-activated (pre-GC) B cells and functions in guiding these cells to the outer follicle[7,8]. EBI2 is down-regulated in GC B cells, a change that is important for GC B cells to access the follicle center[7]. However, in the absence of EBI2, GCs form in their normal location indicating that additional cues must act to promote clustering of GC-precursors at the follicle center.

Sphingosine-1-phosphate (S1P) is a metabolic intermediate made by all eukaryotic cell types during sphingolipid metabolism through the action of sphingosine kinase-1 (sphk-1) and sphk-2[9]. S1P is secreted by some cell types. The extracellular lipid acts as a ligand for any of five G-protein coupled receptors, S1P1–S1P5[9]. Extracellular S1P is abundant (high nM to μM) in blood and lymph but has a half-life shorter than 15 minutes[10] and although no direct measurements of interstitial concentrations have been reported, indirect measurements indicate they are very low[11,12]. Red blood cells and endothelial cells are important sources of circulatory S1P[10,12,13]. Two S1P phosphatases, three lipid phosphate phosphatases (LPPs) and S1P lyase can degrade S1P and catabolism plays a critical role in maintaining the low interstitial concentrations[14]. S1P promotes egress of lymphocytes from lymphoid tissue into circulatory fluids. Whether sufficient amounts of interstitial S1P exist in the lymphoid parenchyma to regulate cell behavior has been unclear.

In this study we set out to define molecular cues involved in regulating GC size and GC B cell clustering. We found that S1P2 was expressed by GC B cells and was necessary to maintain control over the size of chronically-stimulated GCs. S1P2 and its downstream mediators G12, G13 and p115RhoGEF antagonized Akt signaling and cell viability. S1P2 also inhibited GC B cell chemotaxis to follicular chemoattractants and helped to promote confinement of GC B cells to the GC. In addition, S1P2 overexpression in non-GC B cells promoted their localization to the follicle center. Based on these studies, we propose a model in which S1P signals through S1P2 to regulate GC B cell survival and positioning, thus promoting GC homeostasis through dual roles.

Author Manuscript Author Manuscript Author Manuscript Author Manuscript

Results

Uncontrolled growth of S1P2-deficient GCs

Genome-wide comparison of gene expression between follicular and GC B cells identified S1P2 as one of the most strongly induced genes in GC B cells[15] (and data not shown), and this differential expression was confirmed by qRT-PCR (Fig. 1a). When 8–12 week old S1P2-deficient mice[16] were immunized with T-dependent antigens, they appeared to mount GC responses of normal magnitude. However, analysis of one year-old S1P2-deficient mice revealed expansion of GC B cell numbers in mLNs (Fig. 1b) as well as an increase in total B and T cell numbers. In about half the animals GC B cell numbers reached as much as 100× normal, and the architecture of the LN was effaced (Fig. 1b, c). We speculate that the bimodality of GC expansion in these mice is due to cooperation between S1P2-deficiency and secondary genetic events, resulting in a loss of GC homeostasis and development of GC-type lymphoma. Similar observations were made in another S1P2-deficient mouse line and the outgrowths were classified as diffuse large B cell lymphoma (DLBCL)[17]. These results demonstrate a requirement for S1P2 in maintaining GC B cell homeostasis.

Growth advantage of *S1pr2*$^{-/-}$ cells in chronic GCs

To determine if the S1P2-requirement for GC B cell homeostasis was cell intrinsic we studied mixed bone marrow (BM) chimeras. In mice reconstituted with ~1:2 mixtures *of* *S1pr2*$^{-/-}$ and wild-type BM, S1P2-deficient GC B cells over-accumulated relative to their wild-type counterparts in mLNs, whereas follicular B cells were represented in proportion to the BM chimerism (Fig. 1d, e and Supplementary Fig. 1). The outgrowth was even more evident in mice reconstituted with ~1:9 mixtures of *S1pr2*$^{-/-}$ and wild-type BM, and was evident in both mLNs and PPs (Fig. 1f). The outgrowth was not observed in chimeric mice immunized intra-peritoneally with sheep red blood cells (SRBCs) to induce splenic GCs at day 8 post-immunization (Fig. 1e, f) or in splenic or mLN GCs induced 14 days after NP-CGG immunization (Supplementary Fig. 1). However, a gradual outgrowth of S1P2-deficient GC B cells was noted in the endogenous splenic response occurring in unimmunized mixed BM chimeras (Supplementary Fig. 1). This suggests that the outgrowth may depend on the long-term persistence of the GCs rather than on unique properties of mucosal tissues. The advantage for S1P2-deficient cells was dependent on S1P derived from radiation-resistant cells, because it was reduced in polyinosine polycytidylic acid (polyI:C) treated *Mx1-cre*$^{+}$*Sphk1*$^{f/-}$*Sphk2*$^{-/-}$ hosts, animals that lack Sphk2 and are broadly deficient for Sphk1 in IFNα/β-responsive cells (Fig. 1g).

S1P2 can couple to G12 and G13[18]. To test the role of these G-proteins in GC B cells, we generated *Gna12*-deficient mice and intercrossed them with *Gna13*$^{f/f}$ mice[19] carrying the *Mx1-cre* transgene. Animals treated to induce Cre expression were used as a source of G12–G13-double deficient BM cells. In mice reconstituted with a mixture of wild-type and G12–G13-deficient BM, follicular B cells reflected the BM chimerism[20], while there was outgrowth of G12–G13-deficient B cells in mucosal GCs (Fig. 1h). These observations suggest a selective role for G12 and G13 within GC B cells in mediating S1P2 signals. The small GC B cell accumulation seen at day 8 in splenic SRBC responses was similar in the control (G12-deficient) and G12–G13-double deficient groups and may reflect an effect of

Author Manuscript Author Manuscript Author Manuscript Author Manuscript

G12 single-deficiency or influences of genes from the 129 background. A major effector pathway of G12–G13 in lymphocytes is activation of p115RhoGEF (encoded by *Arhgef1*), leading to Rho activation[21–23]. 8–12 weeks after reconstitution with wild-type and *Arhgef1*$^{-/-}$ BM, p115RhoGEF-deficient GC B cells outgrew wild-type cells, although in this case the advantage was not focused in mucosal sites (Fig. 1i and Supplementary Fig. 1). These observations suggest that S1P2 signals through G12–G13 and Rho to maintain B cell homeostasis in chronically stimulated GCs.

S1P2 regulates cell survival in GC B cells

The rate of GC B cell proliferation, determined by measuring bromodeoxyuridine (BrdU) incorporation 0.5 and 6 hr after a single BrdU injection, was similar in S1P2-deficient and control GC B cells (Supplementary Fig. 2). By contrast, the rate of apoptotic cell death, examined *ex vivo* by measuring active caspase-3 and DNA fragmentation was reduced in S1P2-deficient cells (Fig. 2a, b and Supplementary Fig. 2) and in G12–G13-deficient cells (Supplemental Fig. 2). Because S1P2 and Rho were suggested to negatively regulate Akt in some contexts[24–27], we asked whether the activity of this pro-survival kinase was altered in the absence of S1P2. Intracellular flow cytometry for the threonine 308 phosphorylated form of Akt (pAkt T308) showed that S1P2-deficient GC B cells had higher amounts of active kinase than control GC B cells isolated from the same mixed BM chimeras (Fig. 2c). A similar elevation in pAkt T308 was observed after 30 min incubation of wild-type GC B cells with the S1P2 antagonist, JTE-013 (Fig. 2d) or when JTE-013 was added to the media used to prepare the cell suspensions (Supplementary Fig. 2). The cell preparation and incubation was performed in the absence of added S1P, indicating that cells had bound sufficient ligand in vivo or during isolation to promote S1P2 signaling. Co-incubation with the PI3K inhibitor, wortmannin, prevented the increase in pAkt (Fig. 2d). The S1P2-mediated inhibition of Akt activation was dependent on endogenous S1P, because pAkt was elevated in GC B cells from Sphk-deficient mice (Fig. 2e). GC B cells isolated from G12–G13 double-deficient and p115RhoGEF-deficient mice showed similar elevations of pAkt (Fig. 2f). The propensity of wild-type GC B cells to undergo prompt apoptosis *in vitro* limits the biochemical measurements that can be performed in these cells. To assess the S1P2 downstream signals that regulate Akt we used the human GC B cell line, Ramos, which expresses S1P2 (data not shown). Ramos cells had high constitutive pAkt levels, which is not unusual for transformed cell lines (Fig. 2g). Exposure of these cells to S1P led to a reduction in pAkt, which was prevented by co-incubation with the S1P2 antagonist (Fig. 2g). Treatment with Y27632, an inhibitor of the Rho downstream effector ROCK, prevented S1P from causing the full reduction in pAkt levels (Fig. 2h, i). ROCK can inhibit Akt by activating PTEN, a phosphatidylinositol-3,4,5-triphosphate 3-phosphatase[28]. However, incubation in the presence of the PTEN inhibitors bpV(pic) (Fig. 2h), bpV(phen) or VO-OHpic (not shown) did not prevent the S1P-mediated down-modulation of pAkt (Fig. 2h). These observations suggest that upon GC B cell encounter with S1P, S1P2 acts via G12–G13 and p115RhoGEF triggered activation of Rho and ROCK to antagonize Akt activation.

Akt activation confers an advantage in mucosal GCs

To address if elevated Akt activity was sufficient to give GC B cells a growth advantage, BM cells were transduced with a constitutively active *myr-Akt*[29] or control retrovirus and

Author Manuscript Author Manuscript Author Manuscript Author Manuscript

used to reconstitute wild-type mice. Stem cells harboring the *myr-Akt* construct were inefficient at generating follicular B cells, but there was enrichment for myr-Akt expressing cells within the mLN GC compartment (Supplementary Fig. 3). In animals receiving BM cells from *Cr2-cre* transgenic mice transduced with a flox-stop-flox modified version of the *myr-Akt* construct (containing a Thy1.1 reporter) resulting in mature B cell-restricted expression, follicular B cell reconstitution was more successful. The myr-Akt expressing cells were enriched within the GCs of mucosal lymphoid tissues (Fig. 3a) and GC B cells showed a reduced rate of apoptotic cell death (Fig. 3b). These results suggest that increased Akt activation is sufficient to confer a growth advantage on GC B cells.

Akt can promote cell viability by a number of pathways, including phosphorylation and inhibition of the pro-apoptotic molecule Bad, inhibition of Foxo transcription factors that induce pro-apoptotic molecules such as Bim and phosphorylation and inhibition of the translation initiation inhibitor, 4E-BP1, which lead to small increases in cap-dependent translation of many proteins including some pro-survival molecules[30]. Analysis of mice reconstituted with a mixture of wild-type and Bad-deficient BM did not reveal a growth advantage for Bad-deficient GC B cells (Supplementary Fig. 3) and gene expression analysis of sorted wild-type and S1P2-deficient GC B cells failed to reveal differences in expression of Foxo target genes such as Bim (Supplementary Fig. 3). Intracellular staining revealed elevated amounts of phosphorylated 4E-BP1 in S1P2-deficient GC B cells (Fig. 3c). To directly test whether loss of S1P2 signaling promoted translation in GC-type B cells, we measured ^{35}S-cys/met incorporation in Ramos GC B cells. In the absence of S1P, or in the presence of the S1P2 antagonist, ^{35}S-cys/met incorporation by Ramos cells was increased (Fig. 3d). The translation inhibitory effect of S1P2 signaling was similar in magnitude to that achieved by rapamycin, an mTOR inhibitor (Fig. 3d). These findings suggest that S1P2 signaling in GC B cells normally suppresses Akt and thus mTOR activity, leading to reduced 4E-BP1 phosphorylation and a reduction in cap-dependent translation, which may affect the translation of a number of pro-survival molecules[30].

S1P2 regulates GC B cell migration and positioning

S1P2 coupling to Rho activation is associated with inhibition of migration in a number of cell types[31,32]. To test the impact of S1P2 on GC B cell migration to follicular chemo-attractants, we intercrossed S1P2-deficient mice with *Bcl2* transgenic mice to overcome the rapid *in vitro* death of GC B cells[6]. nM concentrations of S1P inhibited GC, but not follicular B cell migration to CXCL13 and CXCL12 in a manner that could be reversed by co-incubation with S1P2 antagonist (Fig. 4a). The selective action of S1P via S1P2 in inhibiting GC B cell migration was confirmed using S1P2-deficient GC B cells (Fig. 4b). Although GCs continued to form in their normal location in the absence of S1P2, the boundary between the GC and mantle zone was often less defined (Fig. 4c and Supplementary Fig 4). In mixed BM chimeras, S1P2-deficient cells were segregated from wild-type cells and enriched at or beyond the GC perimeter (Supplementary Fig. 5). The segregation was largely reversed in Sphk-deficient hosts (Supplementary Fig. 5). G12–G13 double-deficient GC B cells showed a similar tendency to segregate from wild-type GC B cells (Supplementary Fig. 5). To enable a dynamic analysis of S1P2-deficient GC B cell behavior in the context of wild-type GCs, S1P2-deficient hen egg lysozyme (HEL)-specific

Author Manuscript Author Manuscript Author Manuscript Author Manuscript

Hy10 B cells and ovalbumin (OVA)-specific OTII T cells were transferred to wild-type hosts that were then immunized with the low affinity duck egg lysozyme (DEL)-OVA antigen complex to induce GC responses[33]. In frozen sections, S1P2-deficient Hy10 B cells were concentrated at the GC perimeter, often appearing to intermingle with IgD^{hi} follicular mantle cells (Fig. 4d). Two-photon microscopy of explanted LNs containing GFP^+ S1P2-deficient Hy10 B cells and CFP^+ wild-type Hy10 B cells revealed many more S1P2-deficient than wild-type GC B cells moving beyond the confines of the GC, as identified by the location of immune-complex laden follicular dendritic cells (FDCs) (Supplementary Movies 1–3). The S1P2-deficient GC B cells moved at higher velocities and with less turning than the wild-type GC B cells (Fig. 4e and Supplementary Fig. 6). As a result, they traveled in straighter paths (Fig. 4f and Supplementary Fig. 6). When the GC surface was defined based on the distribution of naive B cells (Fig. 4g, Supplementary Fig. 6 and Movies 4–6) it was apparent that S1P2-deficient GC B cells had similar velocities and turning angles whether located outside or inside the GC surface (Fig. 4g, h and Supplementary Fig. 6). In contrast, wild-type GC B cells showed a reduced velocity and increased turning when outside the GC surface (Fig. 4g, h and Supplementary Fig. 6). These observations suggest that as GC B cells move beyond the confines of the GC they receive S1P2-mediated signals that inhibit their migration and prompt their turning.

Despite the marked alteration in distribution of S1P2-deficient cells in the context of a predominantly wild-type GC, we did not observe effects on affinity maturation (Supplementary Fig. 7). This suggests that under the immunization conditions used here, S1P2-deficient cells continued to gain adequate access to antigen and helper T cells. This does not exclude the possibility that during the response to some antigen types, S1P2-deficient cells will exhibit defects in affinity maturation.

S1P2 promotes GC cell clustering

GCs continue to form in S1P2-deficient mice and although S1P2-deficient cells extend beyond the normal GC boundary, they do not disperse freely throughout the follicle, suggesting that additional cues promote their GC association. While the nature of these cues remains undefined, we considered the possibility that removal of general follicular organizing factors might produce a hypomorphic state that could better reveal the confining activity of S1P2. CXCL13 is abundant in the follicle and GC light zone and immunized CXCL13-deficient mice have smaller, less organized GCs than wild-type mice but do retain these structures[6] (Fig. 5a). S1P2-deficient GC B cells failed to form GC clusters in immunized CXCL13-deficient hosts (Fig. 5a). Instead, the $GL7^{hi}$ GC B cells were dispersed throughout the lymphoid areas (Fig. 5a). In another approach, mice were pretreated with an antagonist of lymphotoxin (LT)-$\alpha 1\beta 2$ for 3 weeks to disrupt follicular stromal cell networks[34] prior to SRBC immunization. This treatment also led to a marked dispersal of S1P2-deficient compared to wild-type GC B cells (Fig. 5b). These data suggest that when GC organization is compromised by removing CXCL13 or altering follicular stromal cells, S1P2 plays a non-redundant role in promoting GC B cell clustering. The data also establish that S1P2 promotes GC B cell clustering by a mechanism beyond inhibition of the CXCL13 response.

Author Manuscript Author Manuscript Author Manuscript Author Manuscript

B cells are capable of regulating S1P levels

The interstitial S1P concentrations in the lymphoid tissues are low compared to the high amounts in circulatory fluids but are not precisely defined and may vary between different parts of the tissue[9,35,36]. Although it is not possible to directly measure interstitial S1P, the extent of S1P1 down-modulation from the surface of cells has provided an indirect measure[11,12]. According to the staining levels of an anti-mouse S1P1 monoclonal antibody, wild-type follicular B cells express S1P1 at levels intermediate between blood B cells (that are exposed to μM S1P[9]) and B cells from S1P-deficient mice (Fig. 6a). By comparison with the amounts of S1P needed to cause partial down-modulation of S1P1 in lymphocytes *in vitro*[11], it can be approximated that the follicle contains interstitial S1P in the low nM range. These amounts are sufficient to reduce migration of S1P2-expressing cells to chemokines (Fig. 4a).

Analysis of S1P-degrading enzyme transcript abundance revealed that B cells expressed most of the enzymes that degrade extracellular S1P and, in comparison to T cells, they had especially high amounts of *Lpp2* and *Lpp3* (Fig. 6b), which have their active site in the extracellular region[14]. Incubation of S1P with purified B cells or T cells led to rapid degradation of the lipid by B cells (Fig. 6c). Because the source of extracellular S1P seemed to be radiation-resistant and thus likely stromal cells (Fig. 1g), we next asked whether FDCs, the main radiation resistant cell type present in the center of follicles and within GCs, were a necessary source of S1P. Deletion of *Sphk1* (in *Sphk2*-deficient mice) in FDCs using *Cr2-cre* did not prevent the growth advantage of S1P2-deficient mLN GC B cells and S1P2-deficient cells remained segregated from wild-type GC B cells (Supplementary Fig. 5). This indicated that FDCs are not a required source of S1P for mediating S1P2 functions in GC B cells. These combined findings suggest that extracellular S1P derives from stromal cells outside the follicle center and that it is rapidly degraded as it travels through the follicle, leading us to propose that interstitial S1P concentrations will be lowest in the follicle center.

S1P2 directs B cells to the follicle center

If our hypothesis regarding S1P distribution were correct, cells expressing S1P2 might be antagonized in their migration to chemoattractants in the outer follicle. In consequence, S1P2 expression should favor migration toward the center of the follicle (Supplementary Fig. 8). To test this possibility, we examined the distribution of transferred S1P2-expressing B cells in GC-containing follicles (Fig. 7a). Transduction of B cells with S1P2 led to their preferential clustering around GCs compared to cells transduced with a control vector (Fig. 7a). S1P2 overexpression was also sufficient to cause occasional clustering of the transferred cells in the center of primary follicles (that lack GCs), but this result was more variable. B cell activation, which is required for B cells retroviral transduction, results in upregulation of EBI2 (encoded by *Gpr183*), a receptor that guides B cells to the outer follicle[8]. We considered the possibility that increased EBI2 function might favor movement of the transduced B cells to the outer follicle and thus counteract the effect of S1P2 expression. *Gpr183*$^{+/-}$ B cells express about half as much *Gpr183* as wild-type B cells (Supplementary Fig. 5). Transferred *S1pr2*-transduced *Gpr183*$^{+/-}$ B cells showed a strong bias for migration to the follicle center (Fig. 7b). Importantly, vector-transduced *Gpr183*$^{+/-}$ cells did not show any bias in their distribution, demonstrating that EBI2 heterozygosity was not sufficient to

Author Manuscript Author Manuscript Author Manuscript Author Manuscript

cause a centering effect (Fig. 7b). Transfer of S1P2 expressing cells to hosts broadly deficient in Sphks did not result in a distribution bias (Fig. 7c), indicating that S1P was the signal required. However, the bias was still observed in hosts selectively lacking Sphks in FDCs (Supplementary Fig. 5). These observations suggest that S1P2 upregulation favors cell movement to the follicle center, likely as a consequence of this being a low point in the S1P field (Supplementary Fig. 8). While considered less likely, the results do not exclude the possibility that S1P2-overexpressing cells preferentially die in the outer follicle compared to the center follicle as a result of differential S1P exposure.

Discussion

Here we demonstrate that S1P2 has a dual role in GC B cells, regulating survival and promoting clustering at the follicle center. We provide evidence that S1P2 acts through a signaling module involving G12–G13, p115RhoGEF, and most likely Rho and ROCK, to dampen Akt activation in GC B cells. When S1P2 is lacking, elevated Akt activity can lead to increased phosphorylation of 4E-BP1, a modification that releases this inhibitor from eIF4E, allowing for small increases in cap-dependent translation of a range of transripts[37]. 4E-BP1 regulates translation of transcripts with complex 5'UTRs, including those for a number of pro-survival molecules[38–40]. Our data do not exclude the possibility that Akt promotes GC B cell survival through additional pathways, such as regulation of GSK3 or Glut1[41]. S1P2 can signal via Akt-independent pathways [31,32] and it is possible that their reduction also contributes to the growth advantage observed in S1P2-deficient cells.

Although the *ex vivo* analysis suggests a strong prosurvival effect of S1P2-deficiency, the *in vivo* advantage only becomes evident over periods of weeks in chronically stimulated GCs. This suggests that S1P2's contribution is relatively small during acute antigen-driven GC responses, while it is more strongly revealed under the conditions associated with cell isolation. This may be a consequence of GC B cell exposure to the higher amounts of S1P present outside the GC during tissue preparation as well as the stresses of in vitro culture. We suggest that S1P2's contribution *in vivo* may become most evident under conditions of elevated genotoxic stress arising due to chronic GC stimulation at mucosal sites. The survival advantage may increase the likelihood of cells acquiring and surviving secondary oncogenic hits, thereby setting the stage for progression to DLBCL. Gq negatively regulates Akt activation in naïve B cells[42], indicating that multiple GPCRs exert a controlling influence over Akt activation in B cells. B cells with elevated Akt activity due to PTEN deficiency or Akt over-expression were reported to have reduced isotype switching as a result of decreased activation induced cytidine-deaminase (AID) function[43,44]. We did not observe defects in isotype switching or affinity maturation in S1P2-deficient Hy10 B cells, suggesting AID function is intact. These differences may reflect a lesser increase in Akt activity in S1P2-deficient compared to PTEN-deficient B cells, or they may indicate differences in the way distinct pools of activated Akt are integrated into downstream signaling networks[45].

S1P has a well-established role in promoting lymphocyte egress from lymphoid tissues[9,12]. The present findings establish that S1P also has a role in regulating cell behavior within lymphoid tissue. Follicular S1P is derived from radiation resistant cells other than FDCs and

Author Manuscript Author Manuscript Author Manuscript Author Manuscript

is rapidly degraded by B cells. S1P has a half-life in plasma shorter than 15 minutes[10]. Given that the most frequent cells in blood (red blood cells) do not express S1P degrading enzymes[9] whereas B cells do, it seems likely that the S1P half-life in densely packed B cell follicles will be at least this short.

We propose a model where S1P concentrations are relatively high in the outer follicle and decay to a low point over the FDC network at the follicle center. We suggest that S1P2 induction in GC-precursor cells, by inhibiting their propensity to migrate towards CXCL13 and other attractants in the $S1P^{high}$ outer follicle, helps to focus the cells to the follicle center. S1P2 may also act by promoting chemorepulsion[46], though we have not found GC B cells to move away from S1P in transwell migration assays. EBI2 down-regulation is also important in allowing GC cells to move away from the outer follicle[7]. Once a GC forms, S1P within this microenvironment may be kept at low levels by local degradation and by minimal carriage of S1P into the structure by newly arriving cells. When an S1P2-expressing GC B cell reaches the GC perimeter it likely encounters higher amounts of S1P, causing activation of Rho at the leading edge, prompting retraction of cellular processes[47] and cell turning. Because S1P2 signaling also causes Akt inhibition, this growth-regulatory effect may be strongest in GC B cells migrating near the GC perimeter. Thus, through dual growth regulatory and migration inhibitory activities, S1P2 may act as one of multiple factors that helps link GC size to the volume of the supportive niche at the follicle center. In future studies it will be important to develop techniques to measure interstitial S1P concentrations in order to have a better understanding of how S1P2 could be controlling both processes. Nevertheless, we feel it reasonable to suggest, based on the existing data, that a general property of G12–G13-coupled receptors may be to help coordinate niche confinement and cell survival.

Methods

Mice and immunizations

C57BL/6 and B6-CD45.1 mice were from the National Cancer Institute or Jackson Laboratories. *S1pr2*$^{-/-}$ mice[16] were either seven generations to B6 or on a B6/129 background. BM chimeras[7] were with B6 donors while experiments in *S1pr2*$^{-/-}$ mice were on the mixed background. To generate the *Ga*$_{12}$*-lacZ* knockin allele, *Gna12* gene fragments were from BAC-4922.1. The 5' arm contained 2.8 kb of 5' sequence and the first coding 51bp of exon 1 joined in-frame to a *lacZ*-Sv40polyA cassette followed by a floxed neo cassette (*neo*^{r}). A 2.2 kb 3' arm comprised of exon 1 (26 bp) and intron 1 was inserted between the neo and thymidine kinase (*tk*) cassette. Mice were generated from a clone of targeted RF8 ES cells. The *neo*^{r} cassette was excised by crossing to β-actin-Cre mice. The G12–G13-deficient mice were *Gna12*$^{-/-}$, *Gna13*$^{fl/fl}$ [19], and *Mx1Cre-tg*$^{+/o}$ (on a 129SV/B6 mixed background, MGI 2176073), and were treated neonatally with poly(I:C). The *Rosa26-YFP* locus was introduced as a genetic marker of Cre activity. Sphk1/2-deficient mice[12] were *Sphk2*$^{-/-}$*Sphk1*$^{f/f\ or\ f/-}$ *Mx1-cre-tg*$^{+/o}$ mice that had been treated with poly(I:C) at day 3–5 after birth. *Arhgef1*$^{-/-}$ [48], *Gpr183*$^{+/-}$ [7], HEL-specific MD4 tg (MGI 2384162) and Hy10 mice (MGI 3702699), and *CXCL13*$^{-/-}$ (MGI 2384500) mice were from an internal colony. *Cr2-cre tg* mice (MGI 3047571) were from Klaus Rajewsky. BAD-deficient (MGI

Author Manuscript Author Manuscript Author Manuscript Author Manuscript

2675966) BM was provided by Nika Danial (Dana-Farber). LTβR-Fc (provided by J. Browning, Biogen Idec) was injected i.v. once per week for 4 weeks in doses of 100 μg. NP-CGG (Solid Phase Sciences) immunizations were i.p. (50μg) in Alhydrogel (Accurate Chemical and Scientific Corp.). DEL-OVA immunizations were as previously[33] in Sigma Adjuvant System. SRBC immunizations were i.p. injections of 2.5×10^8 SRBC in Hank's BSS. Animals were housed in specific pathogen-free environment in the Laboratory Animal Research Center at UCSF and all experiments conformed to ethical principles and guidelines approved by the UCSF Institutional Animal Care and Use Committee.

Cell isolation and flow cytometry

B cells from spleen, LNs and PPs were isolated and stained as previously[33]. For detection of surface S1P1, we used a rat monoclonal anti-mouse S1P1 antibody that is under development at R&D Systems. For detection of active caspase-3, 3×10^6 cells were stained for GC markers in 5mL polystyrene tubes, washed, and incubated for 40min at 37°C with FITC-DEVD-FMK (Biovision) in staining buffer (PBS 2% fetal bovine serum (FBS), 1mM EDTA, 0.1% sodium azide) then washed in Caspase Wash Buffer (Biovision). For TUNEL assays, 5×10^6 cells were incubated in RPMI1640 2% FBS for 3 hr at 37°C in 5mL polystyrene tubes. Cells were then fixed with 2% paraformaldehyde (Electron Microscopy Sciences) for 10min at 37°C, washed once in PBS, permeabilized in ice-cold methanol for 30min on ice, then washed and stained for DNA fragmentation as per the manufacturer's protocol (APO-BRDU Apoptosis Detection Kit; BD Biociences) and for GC markers. 3–5×10^6 cells prepared in RPMI1640 containing 0.5% fatty acid free (FAF) BSA (EMD Biosciences) were fixed and permeabilized as above, washed twice in staining buffer, and stained for pAkt T308 (9275 Cell Signaling Technology) or p4E-BP1 T37/46 (2855 Cell Signaling Technology) on ice for 45min followed by biotinylated goat anti-rabbit IgG (BD Biosciences) and streptavidin-Qdot605 (Invitrogen) as well as GC markers. Ramos cells were stained similarly, sometimes using streptavidin-APC (Invitrogen). For intracellular analysis of cells expressing Thy1.1, cells were stained with biotinylated anti-Thy1.1 (HIS51; eBioscience) prior to fixation.

Cell culture, inhibitor treatments, metabolic labeling, and chemotaxis

For Akt activation, 3×10^6 spleen or mLN cells in 5mL polystyrene tubes were resuspended in 200μL RPMI1640 containing 0.5% FAF BSA. 10 μM JTE-013 (Tocris Biosciences) and 200 nM wortmannin (Sigma) were added, and cells were incubated for 30min at 37°C before being fixed and stained as above. Ramos cells were washed twice and sensitized for 1 hr in 0.5% FAF BSA media. Cells were pretreated in 10μM JTE-013 or 10μM Y-27632 (Sigma) for 15 min and then with S1P (Sigma) for 5 min. For Western blots, cells were lysed in prewarmed 2X SDS lysis buffer (100 mM Tris pH 6.8, 4% SDS, 10% Glycerol, 2% betamercaptoethanol, and protease inhibitor cocktail (Roche)), ultracentrifuged, separated by SDS-PAGE, and probed with rabbit anti-phospho-Akt S473 (Cell Signaling Technology) and rabbit anti-actin (Sigma). For metabolic labeling, Ramos cells were washed twice, cultured for 90min in RPMI containing 0.5% FAF BSA with 10nM S1P and 10μM JTE-013 or 200nM Rapamycin (MBL International), washed once and plated in 24-well plates in the same conditions. After 45min, ^{35}S-met/cys labeling mix (EasyTag Express35S Labeling Mix; Perkin Elmer) was added. After 30min, cells were washed, lysed, and soluble lysate

Author Manuscript Author Manuscript Author Manuscript Author Manuscript

was loaded into scintillation fluid (EcoLume; MP Biomedicals) and counts measured with a scintillation counter. Transwell assays were as described[6] with cells from Eμ-*Bcl2*-22 crossed mice (MGI 3052827). For measurement of S1P degradation, B cells were enriched from spleens using anti-CD43 or T cells using anti-B220 microbeads (Miltenyi Biotec). 5×10^6 cells were incubated in 250μl RPMI containing 0.5% FAF BSA with 1μM S1P, spun down and 100μl of supernatants were tested for S1P concentrations by measuring downmodulation of Flag-S1P1 in WEHI231 cells[11].

Gene expression profiling

Total RNA was isolated from ~45,000 sorted wild-type CD45.1 and *S1pr2*$^{-/-}$ GC B cells from mixed chimeric mLNs with the RNEasy Micro Kit (Qiagen). RNA was amplified using the Ovation RNA Amplication System V2 (NuGEN) and cDNA fragments were labeled with the Encore Biotin Module (NuGEN). Samples from 3 experiments were then hybridized to the Affymetrix Mouse Gene ST array, stained, scanned, and normalized by the UCSF Gladstone Genomics Core facility. Normalized data were analyzed using dChip software (http://biosun1.harvard.edu/complab/dchip/). Foxo target genes were selected based on[49].

Immunohistochemistry

7μm cryosections were cut and prepared as described[6]. For human CD4 staining, a tyramide kit (TSA Biotin System; Perkin Elmer) was used according. Images were captured with a Zeiss AxioOberver Z1 inverted microscrope.

Retroviral constructs and transductions

Mouse *S1pr2* or the control truncated *Ngfr* were inserted in a retroviral vector containing a cytoplasmic-domain truncated human CD4 reporter[50]. An insert containing a HA tag and the 14-amino acid myristoylation site of human *v-src* at the N-terminus of *Akt1* was inserted into the MSCV2.2 retroviral vector containing GFP downstream of the IRES. This construct was also inserted into a Thy1.1 reporter vector containing a loxP-eGFP-stop-loxP cassette upstream of the insertion site, and BM from *Cr2-cre* mice was transduced. MD4 B cells were transduced as previously[8]. For S1pr2, due to effects on cell viability or homing, ~3-fold more cells were activated and transduced. For BM transductions, donor mice were injected i.p. with 3 mg 5-Fluorouracil (Sigma). BM was harvested after 4 days and cultured in DMEM containing 15% FBS, antibiotics (50 IU/ml penicillin, 50 μg/ml streptomycin; Cellgro) and 10 mM HEPES (Cellgro), supplemented with IL-3, IL-6, and stem cell factor (SCF) (each at 0.1 μg ml^{-1}, Peprotech). Cells were spin-infected twice at day 1 and 2 and transferred to irradiated recipients on day 3.

Two-photon microscopy

Two similar experimental setups were used. In the first, 3000 *S1pr2*$^{+/+}$ or *S1pr2*$^{-/-}$ GFP$^+$ Hy10 B cells were transferred with 3000 CFP+ Hy10 B cells, 100,000 unlabeled Hy10 B cells, and 50,000 OT-II T cells. In the second, *S1pr2*$^{+/+}$ or *S1pr2*$^{-/-}$ Hy10 BM was retrovirally transduced with a GFP-containing vector. After reconstitution of irradiated recipients, 3000 GFP$^+$ and 15,000 GFP$^-$ Hy10 *S1pr2*$^{-/-}$ B cells were transferred along with

Author Manuscript Author Manuscript Author Manuscript Author Manuscript

3000 CFP^+ Hy10 B cells and 85,000 unlabeled Hy10 B cells. At day 6 after DEL-OVA immunization, 2 mg of rabbit anti-PE (Rockland) was injected i.v. and 2 hours later 10μg PE was injected subcutaneously to label FDC networks with PE immune complexes. Alternatively, the mice received 10^7 CMTMR labeled naïve B cells. On day 7, explanted LNs were prepared[33], and imaged with a custom two-photon microscope equipped with a MaiTai Ti-Saphire laser (Spectra-Physics) or Zeiss LSM 7MP equipped with a Chameleon laser (Coherent). Images were acquired with Video Savant (IO industries) or Zen (Zeiss). Videos were processed with a median noise filter. Excitation wavelength was 910 nm. Emission filters were 570–640 nm for PE, 500–550 nm for GFP and 455–485 nm for CFP in the custom system, or 570–640 nm for PE, 500–550 nm for GFP, and 450–490 nm for CFP in the Zeiss system. Cell tracks were made with Imaris 5.7.2. ×64 (BitPlane) and corrected manually. The velocities and turning angles of cells between each imaging frame were calculated with MatLab (MathWorks). Annotation and final compilation of videos were with Adobe After Effects 7.0. Video files were converted to MPEG format with AVI-MPEG Converter for Windows 1.5 (FlyDragon Software). The boundary of the GC was traced for each x–y slice according to the positioning of naïve follicular B cells, and then the GC surface was calculated by the 'Contour surface' function of Imaris software.

Statistical analysis

All statistical analysis was with Prism software (GraphPad Software, Inc.). For comparison of two nonparametric data sets (Fig. 4f, g, and i), the Mann-Whitney U-test was used. Otherwise, means of two groups were compared with the two-tailed non-paired Student's *t*-test.

Supplementary Material

Refer to Web version on PubMed Central for supplementary material.

Acknowledgments

The authors thank N. Danial (Dana-Farber) for BAD-deficient bone marrow, J. An for help with the mouse colony, and S. Schwab for critical reading of the manuscript. J.A.G. was supported by an NSF fellowship and J.G.C. is an Investigator of the Howard Hughes Medical Institute. This work was supported in part by the Intramural Research Program of the NIH, National Institute of Diabetes and Digestive and Kidney Diseases (RP) and NIH grants HL65590 and HL44907 to SRC and AI45073 to JGC.

References

1. MacLennan ICM. Germinal Centers. Annu. Rev. Immunol. 1994; 12:117–139. [PubMed: 8011279]
2. Allen CD, Okada T, Cyster JG. Germinal-center organization and cellular dynamics. Immunity. 2007; 27:190–202. [PubMed: 17723214]
3. Fagarasan S, Kawamoto S, Kanagawa O, Suzuki K. Adaptive immune regulation in the gut: T cell-dependent and T cell-independent IgA synthesis. Annu. Rev. Immunol. 2010; 28:243–273. [PubMed: 20192805]
4. Goodnow CC, Vinuesa CG, Randall KL, Mackay F, Brink R. Control systems and decision making for antibody production. Nat. Immunol. 2010; 11:681–688. [PubMed: 20644574]
5. Vikstrom I, et al. Mcl-1 is essential for germinal center formation and B cell memory. Science. 2010; 330:1095–1099. [PubMed: 20929728]

Author Manuscript Author Manuscript Author Manuscript Author Manuscript

6. Allen CD, et al. Germinal center dark and light zone organization is mediated by CXCR4 and CXCR5. Nat. Immunol. 2004; 5:943–952. [PubMed: 15300245]
7. Pereira JP, Kelly LM, Xu Y, Cyster JG. EBI2 mediates B cell segregation between the outer and centre follicle. Nature. 2009; 460:1122–1126. [PubMed: 19597478]
8. Pereira JP, Kelly LM, Cyster JG. Finding the right niche: B cell migration in the early phases of T-dependent antibody responses. Int. Immunol. 2010; 22:413–419. [PubMed: 20508253]
9. Schwab SR, Cyster JG. Finding a way out: lymphocyte egress from lymphoid organs. Nat. Immunol. 2007; 8:1295–1301. [PubMed: 18026082]
10. Venkataraman K, et al. Vascular endothelium as a contributor of plasma sphingosine 1-phosphate. Circ. Res. 2008; 102:669–676. [PubMed: 18258856]
11. Schwab SR, et al. Lymphocyte sequestration through S1P lyase inhibition and disruption of S1P gradients. Science. 2005; 309:1735–1739. [PubMed: 16151014]
12. Pappu R, et al. Promotion of Lymphocyte Egress into Blood and Lymph by Distinct Sources of Sphingosine-1-Phosphate. Science. 2007; 316:295–298. [PubMed: 17363629]
13. Pham TH, et al. Lymphatic endothelial cell sphingosine kinase activity is required for lymphocyte egress and lymphatic patterning. J. Exp. Med. 2010; 207:17–27. [PubMed: 20026661]
14. Spiegel S, Milstien S. Sphingosine-1-phosphate: an enigmatic signalling lipid. Nat. Rev. Mol. Cell Biol. 2003; 4:397–407. [PubMed: 12728273]
15. Luckey CJ, et al. Memory T and memory B cells share a transcriptional program of self-renewal with long-term hematopoietic stem cells. Proc. Natl. Acad. Sci. U. S. A. 2006; 103:3304–3309. [PubMed: 16492737]
16. Kono M, et al. The sphingosine-1-phosphate receptors S1P1, S1P2, and S1P3 function coordinately during embryonic angiogenesis. J. Biol. Chem. 2004; 279:29367–29373. [PubMed: 15138255]
17. Cattoretti G, et al. Targeted disruption of the S1P2 sphingosine 1-phosphate receptor gene leads to diffuse large B-cell lymphoma formation. Cancer Res. 2009; 69:8686–8692. [PubMed: 19903857]
18. Ishii I, Fukushima N, Ye X, Chun J. LYSOPHOSPHOLIPID RECEPTORS: Signaling and Biology. Annu. Rev. Biochem. 2004; 73:321–354. [PubMed: 15189145]
19. Ruppel KM, et al. Essential role for Galpha13 in endothelial cells during embryonic development. Proc. Natl. Acad. Sci. U. S. A. 2005; 102:8281–8286. [PubMed: 15919816]
20. Rieken S, et al. G12/G13 family G proteins regulate marginal zone B cell maturation, migration, and polarization. J. Immunol. 2006; 177:2985–2993. [PubMed: 16920934]
21. Girkontaite I, et al. Lsc is required for marginal zone B cells, regulation of lymphocyte motility and immune responses. Nat. Immunol. 2001; 2:855–862. [PubMed: 11526402]
22. Rubtsov A, et al. Lsc regulates marginal-zone B cell migration and adhesion and is required for the IgM T-dependent antibody response. Immunity. 2005; 23:527–538. [PubMed: 16286020]
23. Siehler S. Regulation of RhoGEF proteins by G12/13-coupled receptors. Br. J. Pharmacol. 2009; 158:41–49. [PubMed: 19226283]
24. Ming XF, et al. Rho GTPase/Rho kinase negatively regulates endothelial nitric oxide synthase phosphorylation through the inhibition of protein kinase B/Akt in human endothelial cells. Mol. Cell. Biol. 2002; 22:8467–8477. [PubMed: 12446767]
25. Wolfrum S, et al. Inhibition of Rho-kinase leads to rapid activation of phosphatidylinositol 3-kinase/protein kinase Akt and cardiovascular protection. Arterioscler. Thromb. Vasc. Biol. 2004; 24:1842–1847. [PubMed: 15319269]
26. Sanchez T, et al. PTEN as an effector in the signaling of antimigratory G protein-coupled receptor. Proc. Natl. Acad. Sci. U. S. A. 2005; 102:4312–4317. [PubMed: 15764699]
27. Schuppel M, Kurschner U, Kleuser U, Schafer-Korting M, Kleuser B. Sphingosine 1-phosphate restrains insulin-mediated keratinocyte proliferation via inhibition of Akt through the S1P2 receptor subtype. J. Invest. Dermatol. 2008; 128:1747–1756. [PubMed: 18219276]
28. Li Z, et al. Regulation of PTEN by Rho small GTPases. Nat. Cell Biol. 2005; 7:399–404. [PubMed: 15793569]

Author Manuscript Author Manuscript Author Manuscript Author Manuscript

29. Ahmed NN, Grimes HL, Bellacosa A, Chan TO, Tsichlis PN. Transduction of interleukin-2 antiapoptotic and proliferative signals via Akt protein kinase. Proc. Natl. Acad. Sci. U. S. A. 1997; 94:3627–3632. [PubMed: 9108028]
30. Engelman JA. Targeting PI3K signalling in cancer: opportunities, challenges and limitations. Nat. Rev. Cancer. 2009; 9:550–562. [PubMed: 19629070]
31. Skoura A, Hla T. Regulation of vascular physiology and pathology by the S1P2 receptor subtype. Cardiovasc. Res. 2009; 82:221–228. [PubMed: 19287048]
32. Michaud J, Im DS, Hla T. Inhibitory role of sphingosine 1-phosphate receptor 2 in macrophage recruitment during inflammation. J. Immunol. 2010; 184:1475–1483. [PubMed: 20042570]
33. Allen CD, Okada T, Tang HL, Cyster JG. Imaging of germinal center selection events during affinity maturation. Science. 2007; 315:528–531. [PubMed: 17185562]
34. Browning JL. Inhibition of the lymphotoxin pathway as a therapy for autoimmune disease. Immunol. Rev. 2008; 223:202–220. [PubMed: 18613838]
35. Pham TH, Okada T, Matloubian M, Lo CG, Cyster JG. S1P1 receptor signaling overrides retention mediated by G alpha i-coupled receptors to promote T cell egress. Immunity. 2008; 28:122–133. [PubMed: 18164221]
36. Sinha RK, Park C, Hwang IY, Davis MD, Kehrl JH. B lymphocytes exit lymph nodes through cortical lymphatic sinusoids by a mechanism independent of sphingosine-1-phosphate-mediated chemotaxis. Immunity. 2009; 30:434–446. [PubMed: 19230723]
37. Ma XM, Blenis J. Molecular mechanisms of mTOR-mediated translational control. Nat. Rev. Mol. Cell Biol. 2009; 10:307–318. [PubMed: 19339977]
38. Mamane Y, et al. Epigenetic activation of a subset of mRNAs by eIF4E explains its effects on cell proliferation. PLoS One. 2007; 2:e242. [PubMed: 17311107]
39. Wendel HG, et al. Dissecting eIF4E action in tumorigenesis. Genes Dev. 2007; 21:3232–3237. [PubMed: 18055695]
40. Hsieh AC, et al. Genetic dissection of the oncogenic mTOR pathway reveals druggable addiction to translational control via 4EBP-eIF4E. Cancer Cell. 2010; 17:249–261. [PubMed: 20227039]
41. Wieman HL, Wofford JA, Rathmell JC. Cytokine stimulation promotes glucose uptake via phosphatidylinositol-3 kinase/Akt regulation of Glut1 activity and trafficking. Mol. Biol. Cell. 2007; 18:1437–1446. [PubMed: 17301289]
42. Misra RS, et al. G alpha q-containing G proteins regulate B cell selection and survival and are required to prevent B cell-dependent autoimmunity. J. Exp. Med. 2010; 207:1775–1789. [PubMed: 20624888]
43. Omori SA, et al. Regulation of class-switch recombination and plasma cell differentiation by phosphatidylinositol 3-kinase signaling. Immunity. 2006; 25:545–557. [PubMed: 17000121]
44. Suzuki A, et al. Critical roles of Pten in B cell homeostasis and immunoglobulin class switch recombination. J. Exp. Med. 2003; 197:657–667. [PubMed: 12615906]
45. Schenck A, et al. The endosomal protein Appl1 mediates Akt substrate specificity and cell survival in vertebrate development. Cell. 2008; 133:486–497. [PubMed: 18455989]
46. Ishii M, Kikuta J, Shimazu Y, Meier-Schellersheim M, Germain RN. Chemorepulsion by blood S1P regulates osteoclast precursor mobilization and bone remodeling in vivo. J. Exp. Med. 2010
47. Carmona-Fontaine C, et al. Contact inhibition of locomotion in vivo controls neural crest directional migration. Nature. 2008; 456:957–961. [PubMed: 19078960]
48. Francis SA, Shen X, Young JB, Kaul P, Lerner DJ. Rho GEF Lsc is required for normal polarization, migration, and adhesion of formyl-peptide-stimulated neutrophils. Blood. 2006; 107:1627–1635. [PubMed: 16263795]
49. Dengler HS, et al. Distinct functions for the transcription factor Foxo1 at various stages of B cell differentiation. Nat. Immunol. 2008; 9:1388–1398. [PubMed: 18978794]
50. Reif K, et al. Balanced responsiveness to chemoattractants from adjacent zones determines B-cell position. Nature. 2002; 416:94–99. [PubMed: 11882900]

Author Manuscript Author Manuscript Author Manuscript Author Manuscript

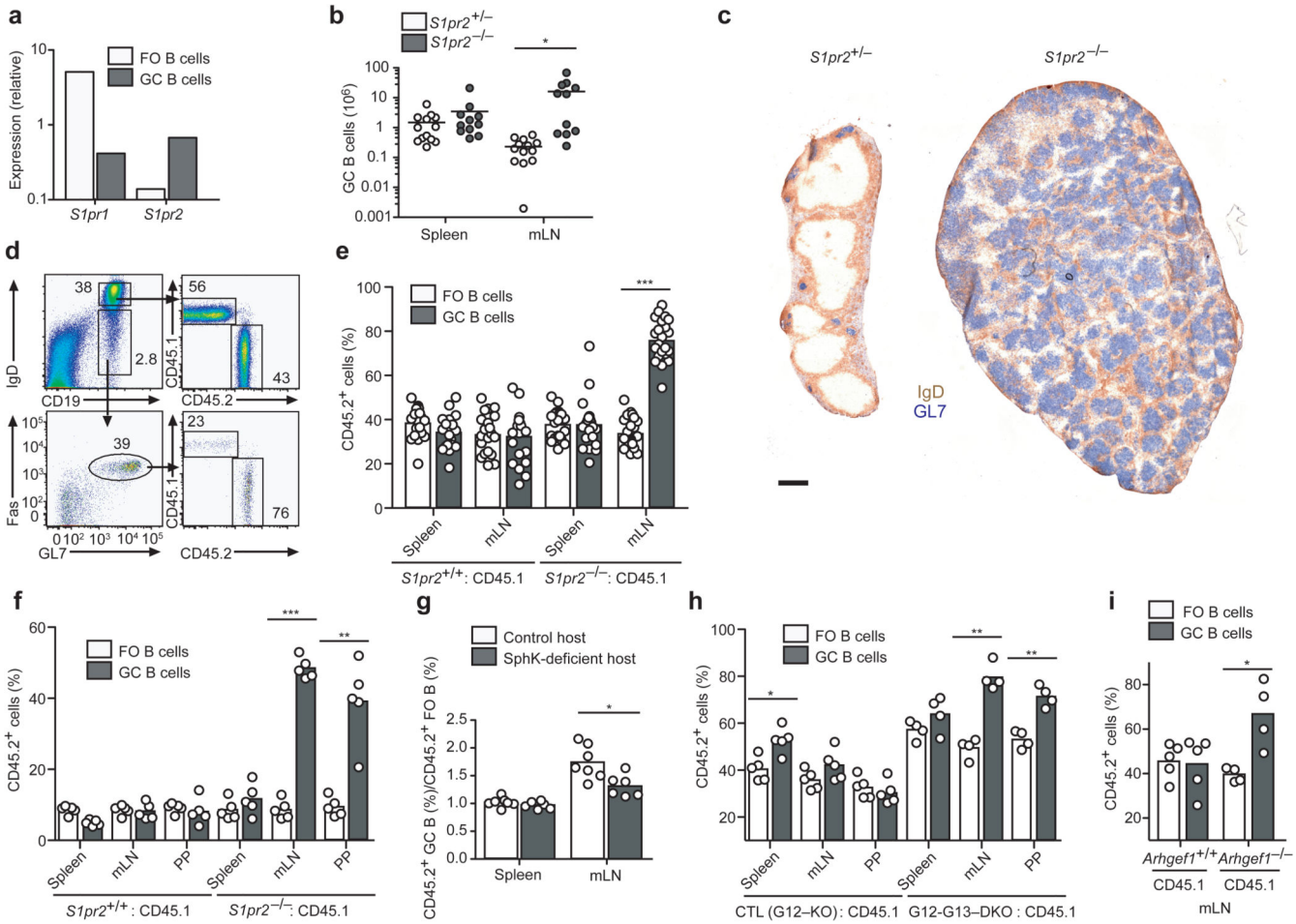

Figure 1. S1P2, G12–G13 and p115RhoGEF-deficient GC B cells have a growth advantage in chronic GCs

(a) Quantitative PCR analysis of *S1pr1* and *S1pr2* transcript abundance in follicular (FO) and GC B cells, shown relative to *HPRT*. (**b)** Number of GC B cells in spleen and mLNs and (**c)** immunohistochemical staining of mLNs from one year-old $S1pr2^{+/-}$ or $S1pr2^{-/-}$ mice. Scale bar, 500 μm. (**d)** Representative flow cytometric analysis of mLN FO and GC populations from 60% wild-type (CD45.1) and 40% $S1pr2^{+/+}$ or $S1pr2^{-/-}$ (CD45.2) mixed BM chimeras. Numbers indicate frequency of cells within gates. **e–f,** Contribution of CD45.2 cells to FO and GC populations in indicated tissues of mixed BM chimeras made with 60:40 (**e**) or 90:10 (**f**) ratios of CD45.1 and CD45.2 BM. In **e**, data are pooled from more than 5 experiments (n = 19–23); **f**, data are representative of 3 experiments (n = 5). (**g)** Relative contribution of $S1pr2^{-/-}$ (CD45.2) GC B cells to GC/FO populations in mixed BM chimeras in $Mx1\text{-}cre^{+}Sphk1^{f/-\ or\ f/f}Sphk2^{-/-}$ hosts. Data are from 3 experiments (n = 6). **h–i,** Contribution of CD45.2 cells to FO and GC populations in indicated tissues of mixed BM chimeras made with ~60:40 ratios of wild-type CD45.1 cells and CD45.2 cells from either littermate controls or mice deficient in G12 and G13 (**h**) or p115RhoGEF (*Arhgef1*) (**i**). Littermate controls in **h** are singly deficient in G12. Data are representative of 2 similar experiments. All chimeras in **d–i** were reconstituted for at least 8 weeks and had been

immunized i.p. with SRBCs 6–8 days prior to analysis. * $P \leq .01$, ** $P \leq .001$, *** $P \leq .0001$.

Author Manuscript Author Manuscript Author Manuscript Author Manuscript

Author Manuscript Author Manuscript Author Manuscript Author Manuscript

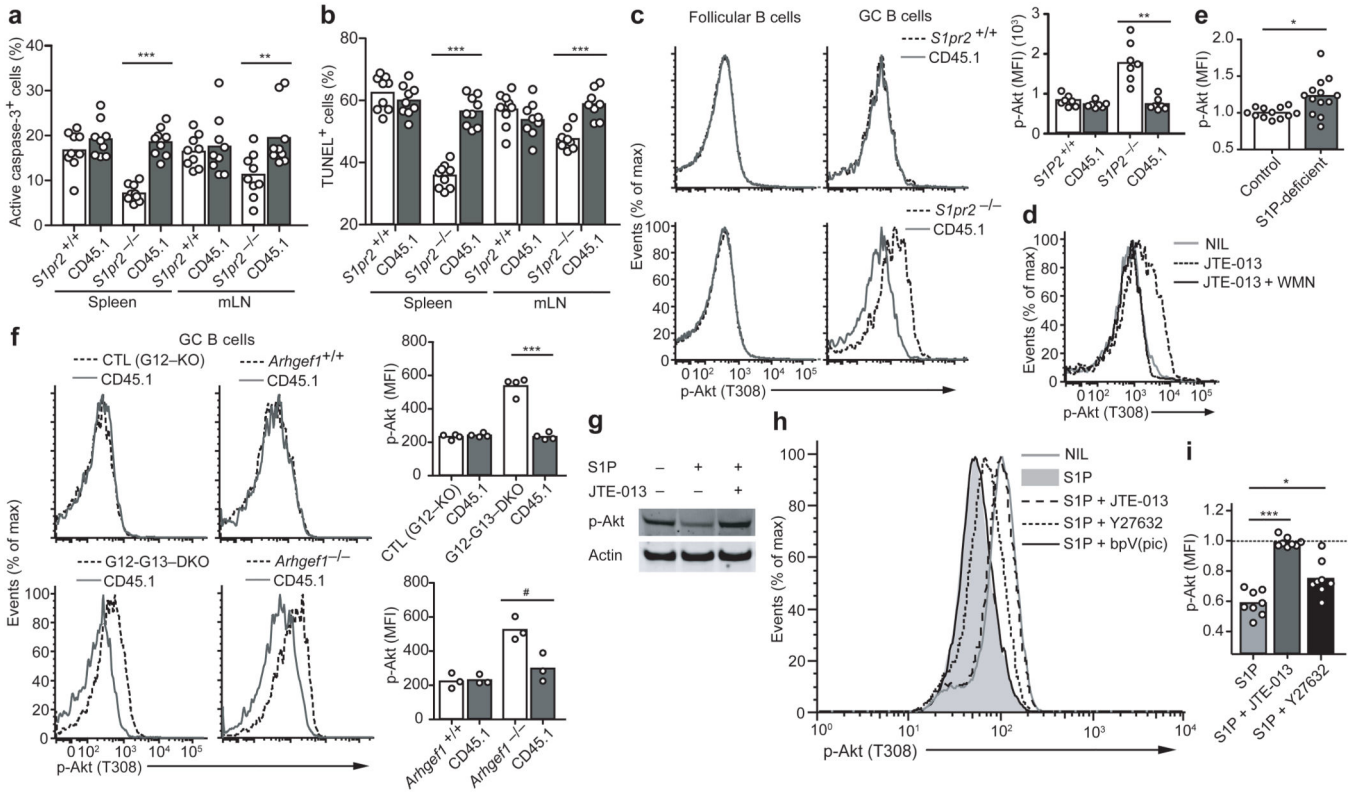

Figure 2. Apoptosis resistance and increased Akt activation in S1P2, G12–G13, and p115RhoGEF-deficient GC B cells

Frequency of GC B cells with activated caspase-3 **(a)** or fragmented DNA detected by TUNEL assay **(b)** in chimeras reconstituted with mixtures of *S1pr2*$^{+/+}$ or *S1pr2*$^{-/-}$ (CD45.2) and wild-type (CD45.1) BM. The mice were immunized with SRBCs and analyzed after 6–8 days. Data are from 3 experiments (n = 8–9). (**c)** Flow cytometric analysis of P-Akt T308 in follicular and GC B cells from mixed chimeras. Right panel shows mean fluorescence index (MFI) of P-Akt T308 in the indicated GC B cell populations (n = 7). (**d)** P-Akt T308 analysis in wild-type GC B cells from spleen suspensions treated with JTE-013 or JTE-013 and wortmannin (WMN) for 30 min immediately *ex vivo* (n = 3). (**e**) Graph showing P-Akt T308 MFI of mLN GC B cells from *Mx1-cre*$^{+}$*Sphk1*$^{f/-\ or\ f/f}$*Sphk2*$^{-/-}$ (S1P-deficient) mice, relative to the average of the controls (n = 12–13, pooled from 6 experiments). (**f)** P-Akt T308 analysis in GC B cells deficient in p115RhoGEF or both G12 and G13, compared to littermate control cells and wild-type (CD45.1) cells, from mixed BM chimeras. The G12–G13 DKO littermate control was G12-single deficient. Right panels show a summary of P-Akt T308 MFIs in GC B cells from mixed chimeras (data are representative of 2 experiments). (**g)** Western blot for P-Akt S473 in Ramos cells treated for 5 min with S1P in the presence or absence of JTE-013 (representative of 3 experiments). (**h**) P-Akt T308 analysis in Ramos cells treated for 5 min with S1P (10nm) alone or in the presence of the indicated inhibitors. Y27632, 10μm; JTE-013, 10μm; bpV(pic), 500nm. (**i**) Relative P-Akt T308 MFIs in Ramos cells treated with the indicated conditions, compared to untreated (dashed line) (n = 8, pooled from 8 experiments). $^{\#}$ $P \leq .05$, * $P \leq .01$, ** $P \leq .001$, *** $P \leq .0001$.

Author Manuscript Author Manuscript Author Manuscript Author Manuscript

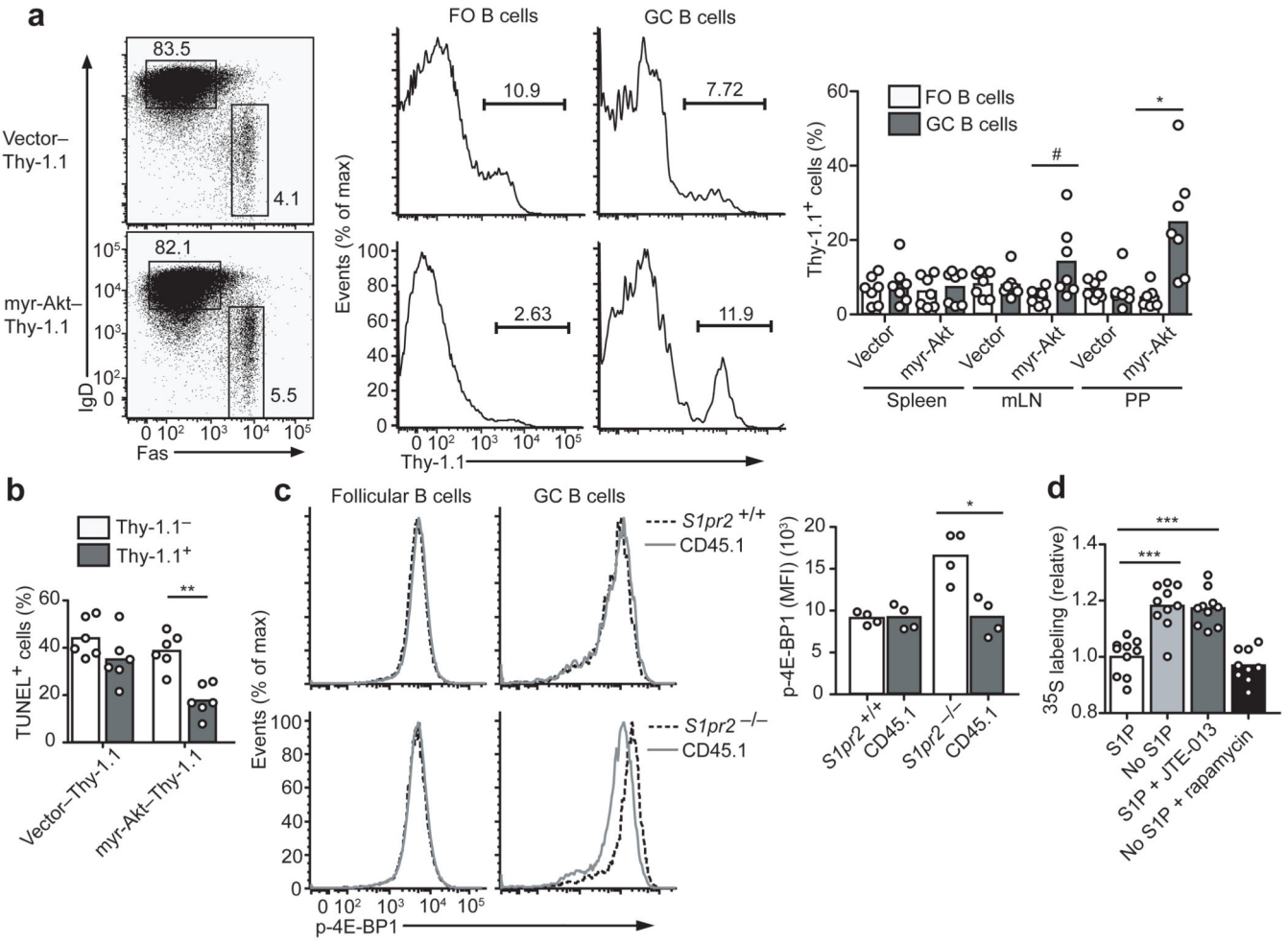

Figure 3. Akt activation confers an advantage in mucosal GCs and S1P2 regulates translation in GC cells

(a) BM from *Cr2-cre* transgenic mice was transduced with loxP-stop-loxP Thy-1.1 control retrovirus (Vector) or myristoylated Akt (*myr-Akt*) Thy-1.1 retrovirus and used to reconstitute irradiated recipient mice. Representative flow cytometric analysis showing representation of myr-AKT–Thy-1.1-expressing cells in IgD^{lo} Fas^{+} GC B cells relative to IgD^{hi} FO B cells of mLNs. Right panel shows summary of data as percent contribution of Thy-1.1^{+} cells to FO and GC B cell populations (n = 7, pooled from 2 experiments). (**b**) TUNEL assay of mLN GC B cells from mice of the type in a. (**c**) Flow cytometric analysis of P-4E-BP1 in FO and GC B cells from mixed BM chimeras containing wild-type (CD45.1) cells and either *S1pr2*$^{+/+}$ or *S1pr2*$^{-/-}$ (CD45.2) cells. Graph on right shows MFI of P-4E-BP1 in the indicated GC populations (n = 4, from 4 experiments). (**d**) Relative incorporation of ^{35}S-labeled cysteine and methionine in 30 min by Ramos cells removed from S1P (No S1P) or treated with JTE-013, relative to cells cultured with S1P. Control samples were removed from S1P and treated with rapamycin. Triplicate measurements were obtained in each experiment and all data points were divided by the mean of the untreated group. $^{\#}$ $P \leq .05$, * $P \leq .01$, ** $P \leq .001$, *** $P \leq .0001$.

Author Manuscript Author Manuscript Author Manuscript Author Manuscript

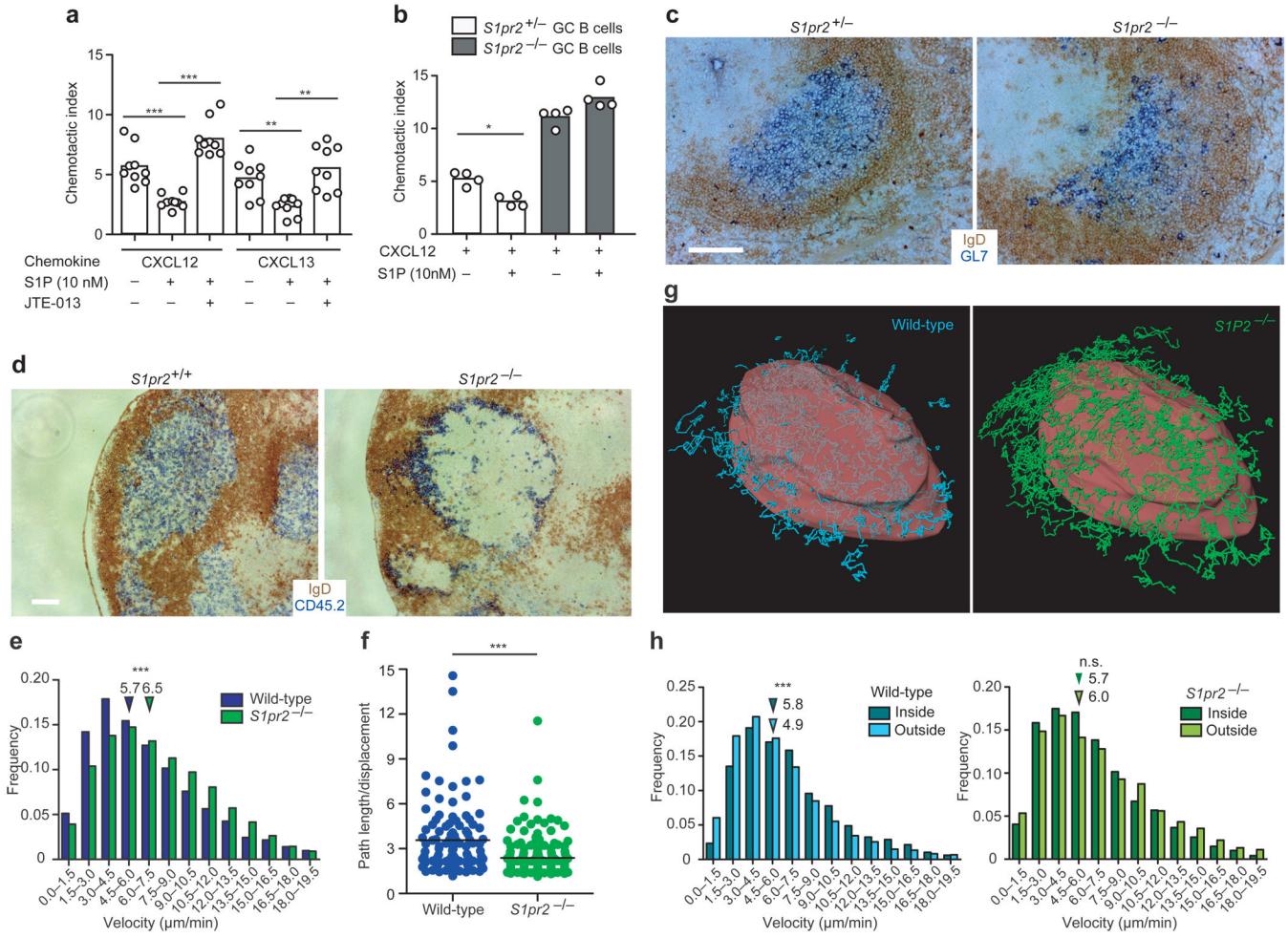

Figure 4. Cell migration and positioning of GC B cells are regulated by S1P2

(a) Transwell migration of wild-type *Bcl2*-transgenic FO and GC B cells to CXCL12 (0.3μg/ml) or CXCL13 (1μg/ml) in the presence or absence of S1P as well as JTE-013 (representative of at least 5 experiments). (**b**) Transwell migration of $S1pr2^{+/-}$ or $S1pr2^{-/-}$ *Bcl2*-transgenic GC B cells to CXCL12 in the presence or absence of S1P (representative of 2 experiments). (**c**) Immunohistochemical analysis of splenic $GL7^{+}$ GCs in $S1pr2^{+/-}$ or $S1pr2^{-/-}$ mice immunized with SRBCs. (**d**) Lysozyme-specific $S1pr2^{+/+}$ or $S1pr2^{-/-}$Hy10 (CD45.2) B cells were transferred into recipient (CD45.1) mice along with wild-type Hy10 (CD45.1) B cells and OVA-specific OT-II (CD45.1) T cells. Recipients were DEL-OVA immunized. At d14 LN sections stained to detect $CD45.2^{+}$ Hy10 GC B cells (blue) and FO B cells (IgD, brown). Scale bar, 200μm. **(e)** Histograms showing velocities of $S1pr2^{+/+}$ and $S1pr2^{-/-}$ GC B cells determined by tracking migration of fluorescently labeled GC B cells using real-time 2-photon microscopy of intact LNs (see also Supplementary Movies 1–2). **(f)** Confinement of wild-type and $S1pr2^{-/-}$ GC B cells, displayed as path length/displacement (data in e and f are representative of 4 GCs analyzed in 2 experiments). (**g**) Example views of GC surface (red) (see also Supplementary Fig. 6) showing tracks of wild-type (CFP^{+}, cyan) and $S1pr2^{-/-}$ GC B cells (GFP^{+}, green) (see also Supplementary Movies 3–6). (**h**) Velocities of GC B cells during migration inside or outside the GC surface. Downward

arrows in e and h denote average values of their respective groups. * $P \leq .01$, ** $P \leq .001$, *** $P \leq .0001$, n.s. $P = 0.73$.

Author Manuscript Author Manuscript Author Manuscript Author Manuscript

Author Manuscript Author Manuscript Author Manuscript Author Manuscript

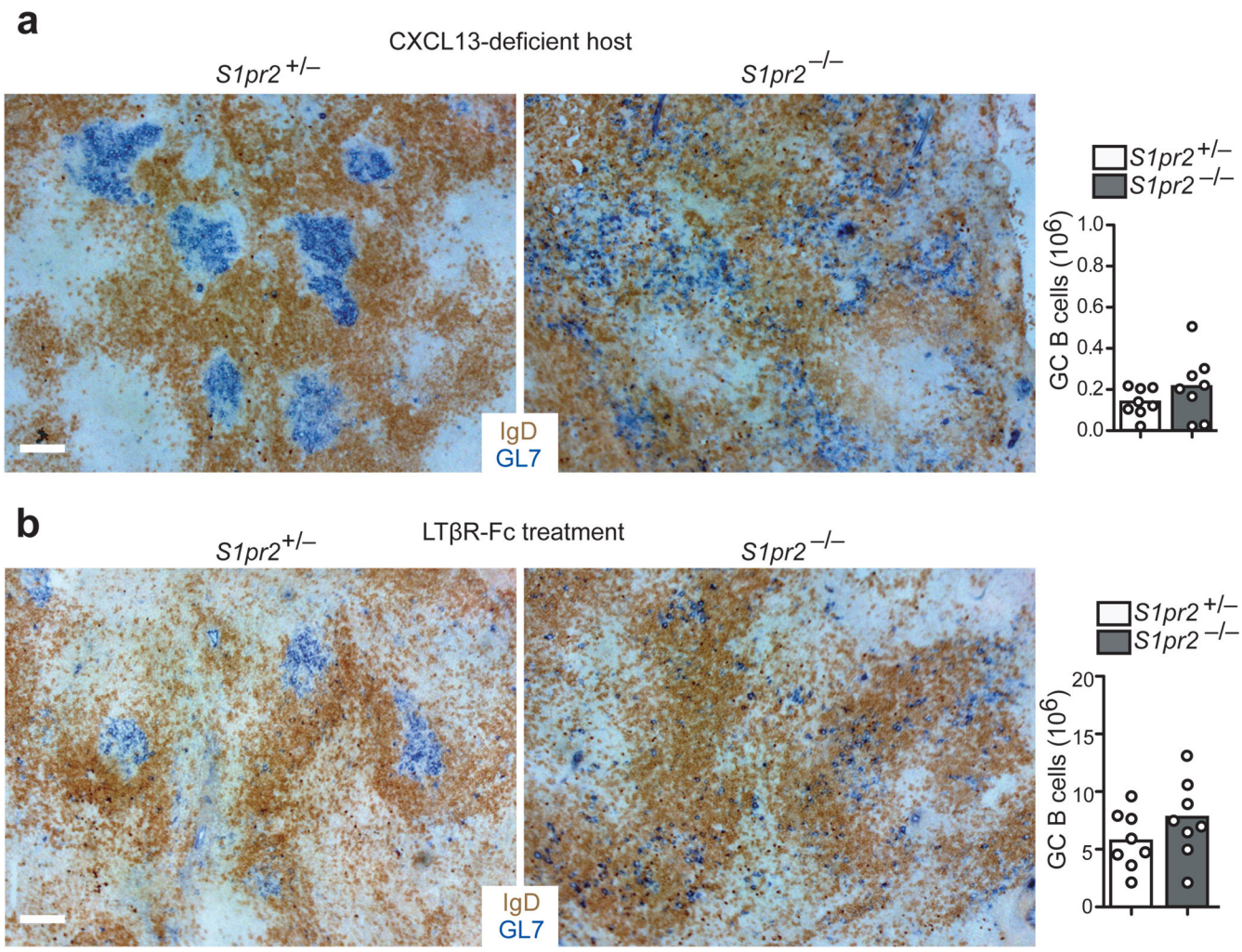

Figure 5. S1P2 cooperates with CXCR5 and FDCs to promote GC B cell clustering

(**a**) Immunohistochemical analysis of mLN sections from CXCL13-deficient mice reconstituted with BM from either *S1pr2*$^{+/-}$ or *S1pr2*$^{-/-}$ donors, showing GL7^{+} GC B cell and IgD^{+} B cell distribution. Right panel shows number of GC B cells per mLN in chimeras (n = 8, pooled from 3 experiments). (**b**) Immunohistochemical analysis of spleen sections from *S1pr2*$^{+/-}$ or *S1pr2*$^{-/-}$ mice treated with LTβR-Fc for 4 weeks. At the fourth injection, mice were immunized i.p. with SRBCs and analyzed 7 days later. Right panel shows numbers of GC B cells in spleen (n = 8, pooled from 3 experiments). Scale bars, 100μm.

Author Manuscript Author Manuscript Author Manuscript Author Manuscript

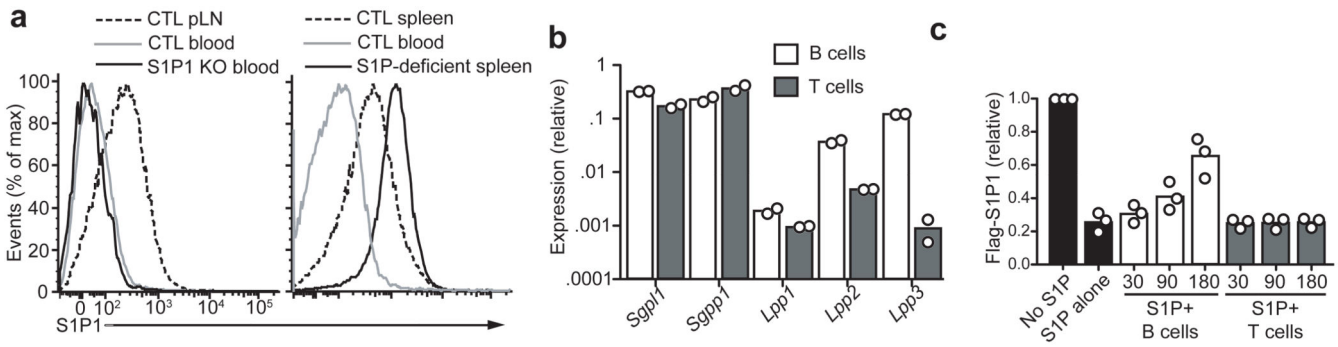

Figure 6. B cells are capable of degrading S1P

(a) S1P1 surface abundance on follicular B cells from the indicated tissues of control (CTL), *S1pr1*-deficient (S1P1 KO), or *Mx1-cre*$^{+}$*Sphk1*$^{f/-\ or\ f/f}$*Sphk2*$^{-/-}$ (S1P-deficient) mice. Data are representative of more than 3 mice of each type. **(b)** Transcript abundance of S1P lyase (*Sgpl*), sphingosine-1-phosphate phosphatase-1 (*Sgpp1*), and lipid phosphate phosphatases (*Lpp*) 1–3 in B cells and T cells, shown relative to *HPRT*. **(c)** Relative amount of S1P remaining in culture supernatants after incubation with B or T cells for the indicated number of minutes, determined by the extent of down-modulation of Flag-S1P1 on a reporter cell line. Data are plotted as MFI of Flag-S1P1 staining relative to reporter cells not exposed to S1P (data are from 3 experiments).

Author Manuscript Author Manuscript Author Manuscript Author Manuscript

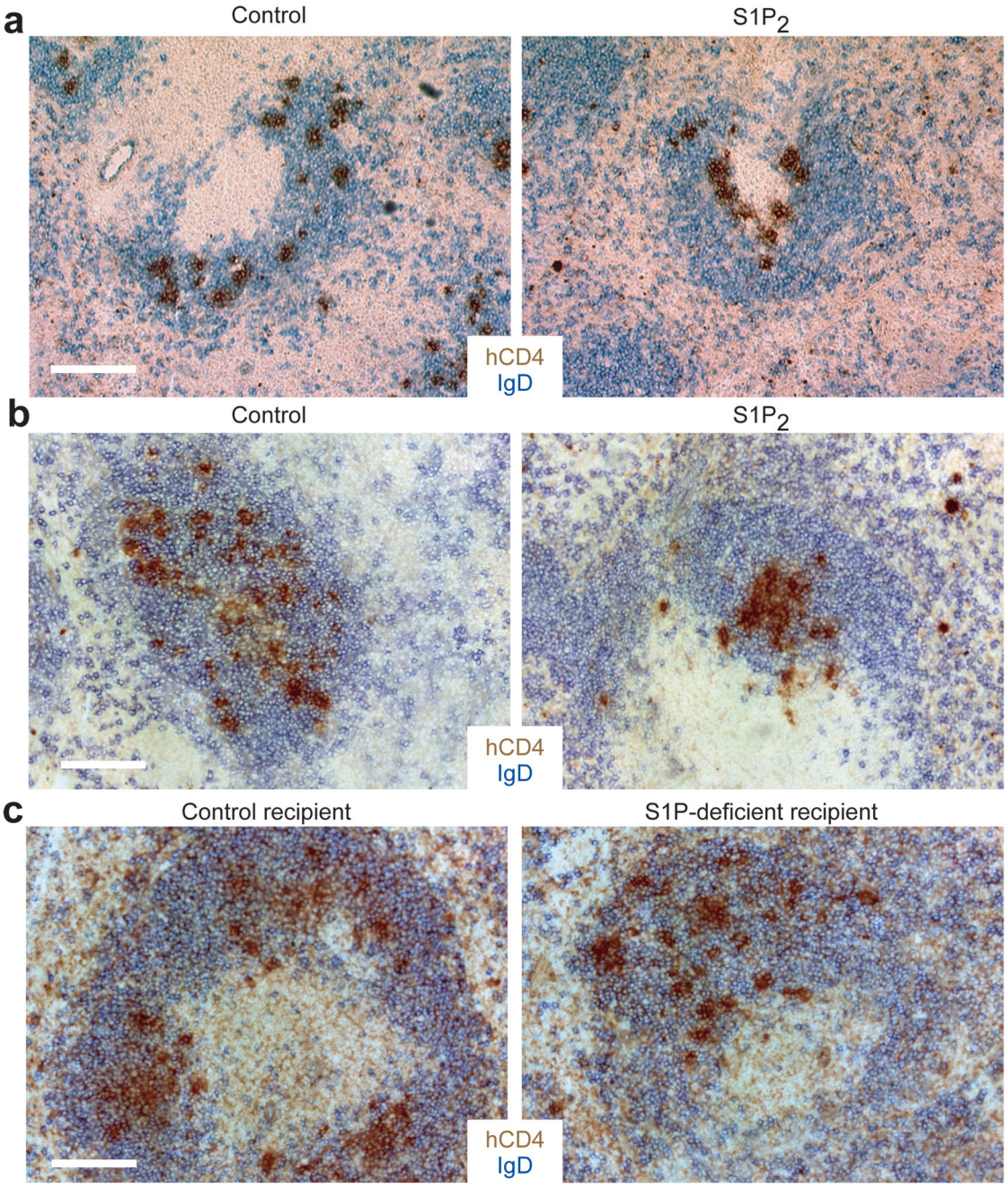

Figure 7. S1P2 directs activated B cells to the GC and the center of the follicle

(a) MD4 B cells retrovirally transduced with vectors encoding either S1P2 or control surface receptor (truncated *Ngfr*) as well as the hCD4 reporter were transferred into day 6 SRBC immunized recipient mice for 24 hours. Immunohistochemical staining of splenic sections shows localization of $hCD4^{+}$ transduced cells in GC-containing follicles. **(b)** S1P2 or control vector transduced $Gpr183^{+/-}$ MD4 B cells were transferred into unimmunized recipients. Immunohistochemical staining shows localization of transduced cells in primary follicles. **(c)** S1P2 transduced $Gpr183^{+/-}$ MD4 B cells were transferred into either littermate control

(*Sphk2*$^{-/-}$) or *Mx1-cre*$^{+}$*Sphk1*$^{f/-\ or\ f/f}$*Sphk2*$^{-/-}$ (S1P-deficient) recipient mice. Immunohistochemical staining shows localization of transduced cells in primary follicles. Data in a–c are all representative of 3 independent experiments. Scale bars, 200 μm.

Author Manuscript Author Manuscript Author Manuscript Author Manuscript